Therefore it is considered that a CO_2 laser (1039 cm^{-1}) will excite the CO stretching mode (1203 cm^{-1}, calculated value of the staggered form; see Figure 7A) or the asymmetric CCO stretching mode (1115 cm^{-1}; see Figure 7B). It is noted that the displacement vectors of these modes correspond to the initial direction of the IRC of process I, where the CO stretching and the CCO angle contracting is remarkable in the early stage of the reaction. Therefore, a CO_2 laser excites the vibrational mode which corresponds to the direction of the reaction path and induces process I selectively.

On the other hand, the HF laser (3644 cm^{-1}) is considered to excite the OH stretching mode (3983 cm^{-1}; see Figure 7C) of ethanol. In the one-step process of II, however, the deformation of the reactant molecule has no contribution of the OH stretching along the IRC. Therefore, the OH stretching mode excited by the HF laser does not play a part as a direct mode to deform the molecule to the direction of the IRC of the one-step process of II. The OH stretching mode interacts with the IRC of process I better than that of the one-step process of II. Because in the reactant region ($s = 4.0$) the displacement vector of the reactant has the component of the OH stretching and the symmetry of the OH stretching mode is C_s, the vibrational energy transfer to the CCO deformation or the asymmetric CCO stretching modes which is expected to interact with the IRC of process I is more effective than that to the asymmetric CH_2 stretching mode (3218 cm^{-1}; see Figure 7D) which is expected to interact with the IRC of the one-step process of II.

Therefore it is considered that the energy supplied by HF laser is effectively used to promote the unimolecular rate process I. This explains well the HF laser enhancement of process I under the condition of low pressure.[13]

Conclusion

In this study we investigated the reaction paths of the unimolecular decomposition of ethanol especially in connection with the mode-selective chemical reactions.

Five unimolecular decomposition paths were analyzed by ab initio MO calculations. The geometries and energies of the reactants, TS's, reaction intermediates, and products have been determined on the singlet PES. The most energetically favorable unimolecular path is the formation of ethylene. With respect to the acetaldehyde formation, the one-step mechanism is more favorable than the two-step mechanism via vinylalcohol. A possible radical formation process is also suggested.

We also discussed the dissociation paths leading to ethylene or acetaldehyde on the basis of "reaction ergodography". We found that the CO stretching or asymmetric CCO stretching modes which would be excited by CO_2 laser correspond to the displacement vector of the IRC for the decomposition to ethylene, so that CO_2 laser highly selects the reaction path to ethylene. Moreover the OH stretching mode excited by HF laser plays a role of energy transfer to the reaction path leading to ethylene.

Acknowledgment. The numerical calculations were carried out at the Data Processing Center of Kyoto University and the Computer Center of Institute for Molecular Science (IMS).

Registry No. Ethanol, 64-17-5.

Microwave Spectroscopic Study of Malonaldehyde. 3. Vibration–Rotation Interaction and One-Dimensional Model for Proton Tunneling

Steven L. Baughcum,[1a] Zuzana Smith, E. Bright Wilson,* and Richard W. Duerst[1b]

Contribution from the Department of Chemistry, Harvard University, Cambridge, Massachusetts 02138. *Received November 18, 1983*

Abstract: Strong perturbations are observed in the microwave spectra of a number of isotopically substituted species of malonaldehyde, all containing deuterium in the hydrogen bond. They are well fitted by using Pickett's reduced axis system (RAS) for the definition of the rotating axes. (Instantaneous principal axes do not fit the data as well and are much less convenient.) The RAS fit gives accurate values for the rate of deuterium transfer between the two oxygen atoms in eight symmetrically substituted isotopic species and in two unsymmetrically substituted species, namely ($D_6D_8{}^{13}C_{2-4}$) and ($D_6D_8{}^{13}C_{2-4}{}^{13}C_3$). The inverse cross product of inertia, F, is also obtained from the fit. An attempt to put rough limits on the height (V_b) and width ($2x_0$) of the barrier separating the two equivalent potential minima was only moderately successful, the barrier height for deuterium tunneling species lying in the range 4.0–5.2 kcal/mol and the separation of the two minima ranging from 0.994 to 0.822 Å for the various isotopic species, as determined from the earlier microwave structure. The effective mass to be used with the pseudo-one-dimensional double-minimum potential function was estimated to be ~1.2 au for the parent species and 2.12 to 2.53 au for the several species with deuterium tunneling. These values were estimated from the experimental values of the *ab* cross term $\langle 0|F|1\rangle$ in the inverse tensor and the tunneling splittings. An alternative approach used the slightly differing tunneling splittings, ΔE_{01}, for a set of symmetrically isotopically substituted species. This latter approach yields also the contribution of each atom to the effective mass. The results indicate that the reaction path near the transition state deviates only a little from parallelism to x_6, the *a* component of the displacement of the proton in the H bond.

Malonaldehyde (3-hydroxy-2-propenal, see Figure 1) is one of the simplest molecules containing a ring closed by a hydrogen bond. It should therefore be a suitable system to investigate in order to extract information about the forces acting in this bond both from the analysis of spectroscopic data and from quantum chemical calculations of various levels levels of approximation.

In the vapor phase, the two equivalent unsymmetrical planar equilbrium configurations shown in Figure 1 have been demonstrated to be present.[2,3] Rapid tunneling occurs between these

(1) (a) Present address: Los Alamos National Laboratory, Los Alamos, NM 87545. (b) Present address: Analytical and Properties Laboratory, 3M Center, St. Paul, NM 55144.

(2) (a) Rowe, W. F., Jr. Ph.D. Thesis, Harvard University, 1975. (b) Baughcum, S. L. Ph.D. Thesis, Harvard University, 1978.

0002-7863/84/1506-2260$01.50/0

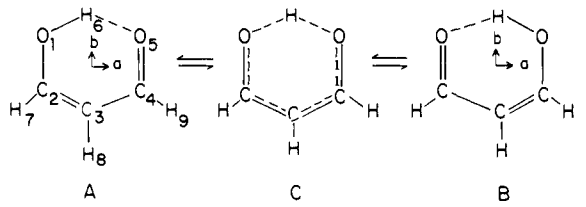

Figure 1. Hydrogen-bonded, tunneling structures of malonaldehyde: A and B, two equivalent equilibrium configurations of malonaldehyde; C, symmetric transition-state structure.

two forms,[2,3] which thus provides an example of hydrogen transfer from one oxygen atom to another via tunneling at rates which can be determined.[2,4]

The quantitative molecular structure has been obtained from the analysis of the microwave spectra of a number of isotopic species[3b] and has been compared with the structures obtained by several quantum chemical studies.[5] Likewise, a reasonably successful analysis[6,7] of the infrared spectra of a few isotopic species has yielded a quadratic force field. Comparisons have been made between calculated and experimental frequencies.[6,8]

Although low J transitions in the microwave spectra of many isotopic species of malonaldehyde can be reasonably well fitted by the usual rigid rotor model, some transitions for certain species show very definite and sometimes large deviations. These have been analyzed[2,3] as being due to perturbations arising from certain terms in the Hamiltonian which couple rotation and vibration more strongly than usual because of the near degeneracy of the two lowest vibrational manifolds arising from the two equivalent equilibrium configurations.

The main purpose of this paper is to present an analysis of these perturbations and the resulting tunneling splittings for a number of isotopic species. Further, these lead to certain conclusions concerning the potential energy surface.

Rotating Axes

As usual, a set of rotating axes is introduced so that the classical Hamiltonian function is described in terms of the Eulerian angles of the rotating axes and the internal coordinates of the nuclei in the rotating axis system.[9] The Hamiltonian can then be written as the sum

$$H = H_V + H_R + H_{VR} \tag{1}$$

where

$$H_V = \sum G_{ij} p_i p_j + V(q_i...) \tag{2}$$

is the vibrational part ($H = H_V$ for $J = 0$) and does not depend on the Eulerian angles. G_{ij} are the usual **G** matrix coefficients[10] except that they are not necessarily constants but may depend on the (internal) vibrational coordinates q_i. The p_i are the momenta conjugate to the q_i. $V(q_i)$ is the potential energy.

The rotational part is

$$H_R = \mu_a P_a^2 + \mu_b P_b^2 + \mu_c P_c^2 + \mu_{ab}(P_a P_b + P_b P_a) + \mu_{bc}(P_b P_c + P_c P_b) + \mu_{ca}(P_c P_a + P_a P_c) \tag{3}$$

where P_a, P_b, and P_c are the components of the total angular momentum of vibration and rotation along the rotating axes a, b, and c while the coefficients μ_a, etc., are functions of the vibrational coordinates q_i and are related to the elements of the instantaneous inertial tensor.[11] The remaining terms are the Coriolis interactions and involve both vibrational coordinates and the angular momentum components P_a etc. The coupling term H_{VR} has the form $L \cdot P$ where **L** is the vibrational angular momentum vector and P is the total angular momentum.[11,12]

This classical Hamiltonian can be converted to a quantum mechanical operator by replacing P_a, P_b, and P_c by the appropriate operators and adding a certain function $V'(q_i)$.[11]

There are various choices for the rotating axes. The G_{ij} are independent of this choice but the terms in H_R and H_{VR} are not. In the present work, instantaneous principal axes of inertia and so called reduced axis system (RAS) axes[11] were tested and the RAS axes were found to fit the observed spectra considerably better. They were also easier to fit to the data, because the values found for the rotational constants, A, B, and C, did not differ greatly for unperturbed and perturbed transitions whereas the differences were large when instantaneous principal axes were employed.

In the instantaneous principal axis system, the terms in H_R which involve μ_{ab}, μ_{bc}, and μ_{ca} vanish identically, whereas L can then have a large contribution from the large-amplitude tunneling coordinate. In RAS axes, on the other hand, the contribution to L of the large-amplitude coordinate, call it q_a, vanishes, but small Coriolis contributions remain from the other, small-amplitude coordinates. Further, the rotating RAS axes do not (except at the equilibrium configuration) always coincide with the instantaneous principal axes so terms such as

$$\mu_{ab}(P_a P_b + P_b P_a) \text{ etc.}$$

in H_R have to be included. These terms will enter only through the second-order and higher perturbation treatment since the diagonal element $(\mu_{ab})_{v,v}$ vanishes.

The Energy Matrix

The energy matrix for H is set up in a basis set of the product form

$$\chi_{vJ} = \Phi_v R_J$$

where Φ_v is an eigenfunction of H_V and is a function of the internal coordinates with quantum number v, which stands for the set v_1, v_2, ... The rotational function R_J depends upon the Eulerian angles and has quantum numbers J, τ, and M, here represented by the single symbol J.

Symmetry. The Hamiltonian H for the normal isotopic form is unchanged by any permutation of identical nuclei and in particular under the permutation $C'_2 = (15)(24)(79)$, i.e., under the simultaneous interchange of these three pairs of equivalent atoms, numbered as in Figure 1. This is a feasible permutation in the sense of Longuet-Higgins,[13] in that this permutation can be accomplished by rotation about the b axis by 180°, followed by the tunneling operation.

The group E, C'_2, where E is the identity operation, therefore leaves H and also H_V invarient and wave functions for H should be classifiable as either even or odd under C'_2. Then

$$\Phi_v R_J \pm C'_2 \Phi_v R_J$$

is a pair of functions (one of which may vanish) even (+ sign) and odd (− sign) under C'_2, respectively.

Nature of the Energy Matrix. The large-amplitude coordinate in RAS axes is here approximately x_6, the displacement of H_6 in the a direction in the molecule plane. The main concern is with the $v = 0$ and $v = 1$ states. The (0,0) block is coupled strongly to the (1,1) block through the matrix element

$$F(P_a P_b + P_b P_a)_{JKM,JK'M}, \; F = \langle 0|\mu_{ab}|1\rangle$$

(3) (a) Rowe, W. F., Jr.; Duerst, R. W.; Wilson, E. B. *J. Am. Chem. Soc.* **1976**, *98*, 4021–4023. (b) Baughcum, S. L.; Duerst, R. W.; Rowe, W. F.; Smith, Z.; Wilson, E. B. *J. Am. Chem. Soc.* **1981**, *103*, 6296–6303. (c) Note that in Table IV of ref 3b the last two isotopic species should have been ($D_6D_7D_8$) and ($D_6D_8D_9$).

(4) Rossetti, R.; Brus, L. E. *J. Chem. Phys.* **1980**, *73*, 1546–1550.

(5) (a) Del Bene, J. E. Kochenour, W. L. *J. Am. Chem. Soc.* **1976**, *98*, 2041–2046. (b) Karlstrom, G.; Jonsson, B.; Roos, B.; Wennerstrom, H. *Ibid.* **1976**, *98*, 6851–6854. (C) Bouma, W. J.; Vincent, M. A.; Radom, L. *Int. J. Quantum Chem.* **1978**, *14*, 767–777.

(6) Smith, Z.; Wilson, E. B.; Duerst, R. W. *Spectrochim. Acta, Part A* **1983**, *39A*, 1117–1129.

(7) Seliskar, C. J.; Hoffmann, R. E. *J. Mol. Spectrosc.* **1982**, *96*, 146–155.

(8) Bicerano, J.; Schaeffer, H. F., III; Miller, W. H. *J. Am. Chem. Soc.* **1983**, *105*, 2550–2553.

(9) Allen, H. C., Jr.; Cross, P. C. "Molecular Vib-Rotors"; John Wiley and Sons, Inc.: New York, 1963.

(10) Wilson, E. B. *J. Chem. Phys.* **1939**, *7*, 1047–1052.

(11) Pickett, H. M. *J. Chem. Phys.* **1972**, *56*, 1715–1723.

(12) Nielson, C. J. *Acta Chem. Scand., Ser. A* **1977**, *A31*, 791–792.

(13) Longuet-Higgins, H. C. *Mol. Phys.* **1963**, *6*, 445–460.

Table I. Measured MW-MW Double Resonances for (D_6D_8)

pump transition (MHz)		signal transition (MHz)	
5_{14}–5_{05} ($v = 1$)	26 047	5_{14}–4_{23} ($v = 1$)	37 383.58
		5_{14} ($v = 1$)–6_{15} ($v = 0$)	36 708.10
6_{42}–6_{33} ($v = 0$)	26 196	6_{51}–6_{42} ($v = 0$)	38 817.0
		5_{41} ($v = 1$)–6_{42} ($v = 0$)	33 721.60
7_{43}–6_{52} ($v = 0$)	23 977	6_{52}–6_{43} ($v = 0$)	39 539.50
		5_{51} ($v = 1$)–6_{52} ($v = 0$)	34 729.76

if the basis functions R_{JKM} are Wang-type symmetric rotor functions. The 0,0 and the 1,1 blocks are also weakly coupled to many other diagonal blocks v,v, but the effect of these can usually be adequately treated by Van Vleck perturbation theory carried through second order. The effect is to alter somewhat the values of the rotational constants A_v, B_v, and C_v and the quartic centrifugal distortion constants. Since all these are adjusted to bring about agreement with the experimental frequencies, these perturbation corrections do not need to be discussed further here.

The off-diagonal coupling elements 0,1 and 1,0 are usually too big to be handled by perturbation theory so the double size 0 and 1 block of H (for each J) was numerically diagonalized. It has the form

$$\begin{vmatrix} A_0P_a^2 + B_0P_b^2 + C_0P_c^2 & F(P_aP_b + P_bP_a) \\ F(P_aP_b + P_bP_a) & A_1P_a^2 + B_1P_b^2 + C_1P_c^2 + \Delta E_{01} \end{vmatrix}$$

where A_0, B_0, and C_0 are the effective rotational constants for the vibrational level $v = 0$, A_1, B_1, and C_1 are the rotational constants for level $v = 1$, and ΔE_{01} is the vibrational energy difference, $v = 1$ minus $v = 0$, i.e., the tunneling splitting. P_a^2 etc. represent the $2J + 1$ by $2J + 1$ matrices for these rotational operators.

Numerical solution of the corresponding secular equation leads to the rotation–vibration energy levels for the $v = 0$ and $v = 1$ rotational manifolds. The experimental perturbed spectrum can be fitted by adjusting eight parameters, namely, A_0, B_0, C_0, A_1, B_1, C_1, F, and ΔE_{01}, neglecting centrifugal distortions.

The choice of RAS axes has caused the vanishing of the $v = 0, v' = 1$ off-diagonal terms of $L \cdot P$ arising from the large-amplitude motion.

Determination of Tunneling Splitting in Malonaldehyde

A large number of microwave transitions for 29 isotopic species were measured, assigned, and reported earlier (ref 3b and associated supplementary material). Transitions of many species with deuterium in the hydrogen bond were fitted with the computer program CORFIT.[14] A slightly modified version is listed in ref 2b, which also gives some practical measures for carrying out this eight-parameter linearized least-squares fit.

In some cases (including the normal isotopic form) the splitting ΔE_{01} is large enough and the off-diagonal coupling terms small enough so that the unmodified rigid rotor model fits the data for low J levels quite well, as could be expected if a second-order perturbation treatment were adequate. In the extreme case this situation would permit only the six effective rotational constants to be determined plus ten centrifugal distortion constants and in less extreme cases also the value of $F^2/\Delta E_{01}$ but not F and ΔE_{01}, separately. It could then happen that the spectrum was fitted very well but not with a unique determination of the rotation–vibration parameters. However, in paper 4 the successful analysis of the microwave spectra of the parent species is described as well as an improved analysis of data for (D_6D_8) and ($D_6D_8{}^{13}C_2{}^{13}C_3{}^{13}C_4$).

Transitions from a state of the $v = 0$ rotational manifold to one in the $v = 1$ manifold are dependent on the small ($\sim$0.3 D)[3b,c] a component of the permanent dipole moment of the molecule in one of its equilibrium configurations. It would therefore be extremely difficult to find intersystem transitions without accurate predictions of their frequencies.

With the aid of the predictions based on the analyses of the rather large (as large as 8 GHz) perturbations found in (D_6D_8), three intersystem transitions were measured by frequency-modulated microwave–microwave double resonance. The double-resonance pump was first checked by tuning to a pure rotation transition within a single tunneling state and then measurement was made of the intersystem transitions. See Table I and Figure 2. The agreement of the observed frequencies with those predicted is very satisfying and provides strong evidence for the validity of the parameters, especially the tunneling splitting ΔE_{01}, extracted from the analysis.

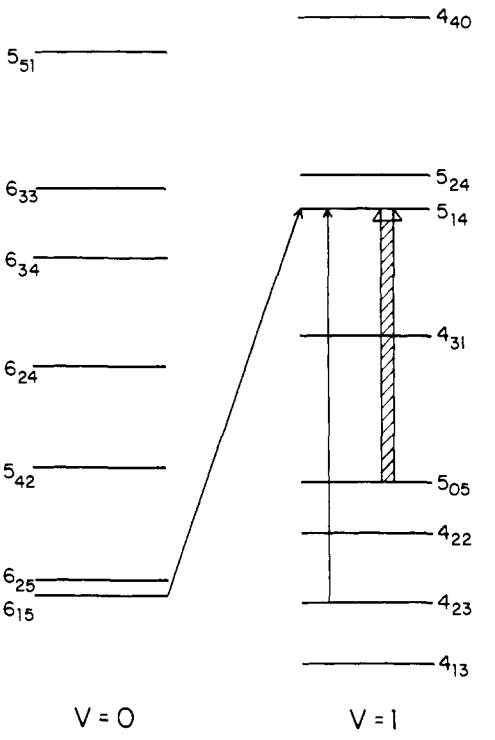

Figure 2. Energy level diagram for the measurement of a rotation–vibration transition in (D_6D_8) with use of MW–MW double resonance. The cross-hatched arrow is the double-resonance pump.

Table II. Tunneling Splittings, ΔE_{01}, and the Rotation-Vibration Coupling Constants, F, for Several Isotopic Species of Malonaldehyde

isotopic species	ΔE_{01}, cm^{-1}	F, MHz
(D_6)	2.915 (4)	100.5 (2)
(D_6D_8)	2.88360 (2)	87.9 (1)
(D_6D_8)[a]	2.883576 (3)	87.795 (1)
($D_6D_8{}^{18}O_1{}^{18}O_5$)	2.715 (2)	82.0 (3)
($D_6D_7D_9$)	2.943 (1)	95.7 (3)
($D_6D_7D_8D_9$)	2.909 (1)	84.3 (1)
($D_6D_8{}^{13}C_{2-4}$)	2.862 (1)	85.9 (2)
($D_6D_8{}^{13}C_{2-4}{}^{13}C_3$)	2.842 (1)	81.4 (2)
($D_6D_8{}^{13}C_2{}^{13}C_4$)	2.855 (1)	83.6 (2)
($D_6D_8{}^{13}C_2{}^{13}C_3{}^{13}C_4$)	2.82833 (5)	80.36 (4)
($D_6D_8{}^{13}C_2{}^{13}C_3{}^{13}C_4$)[a]	2.82839 (1)	80.25 (1)
parent[a]	21.583264 (1)	45.51 (4)

[a] The values obtained by using the Nielsen/Halonen program are described in paper 4. The extra decimal places show the agreement between this and the Corfit program.

Table II lists the values of the tunneling splittings for a number of substituted isotopic species containing D_6, all obtained by fitting the perturbations as described above. Note that with the exception of ($D_6D_8{}^{13}C_{2-4}$) and ($D_6D_8{}^{13}C_{2-4}{}^{13}C_3$) the species are symmetrically substituted. For a discussion of quenching of tunneling in unsymmetrically substituted species see paper 2.[3b]

The energy splitting $\Delta E_{01} = 26 \pm 10$ cm^{-1} for the parent isotopic species was earlier estimated from relative intensity measurements.[2b] In order to obtain an accurate value from deviations from rigid rotor frequencies, it is necessary to go to higher J transitions for which centrifugal distortion terms in the Hamiltonian must be included. The accurate value for the parent species was found

(14) Pickett, H. M., Jet Propulsion Laboratory, California Institute of Technology, Pasadena, CA 91109.

to be (see paper 4) $\Delta E_{01} = 21.583\ cm^{-1}$.

One-Dimensional Potential Function

Molecules with two equivalent equilibrium configurations arising from puckering vibrations of four- and five-membered rings[15] have been successfully treated by simple one-dimensional models with a constant effective mass, m_o, so it is reasonable to try such an approximation here.[16] It turns out to be only moderately successful.

A simple form for the one-dimensional double-minima potential energy V is

$$V = \tfrac{1}{2}kx^2 + ax^4 \tag{4}$$

where x is the effective coordinate, expected to be nearly equal to x_6, the a coordinate for the tunneling hydrogen. k and a in eq 4 are parameters, k being negative. The energy minima are at $x = \pm x_o$ with $x_o = (1/2)(-k/a)^{1/2}$, and the barrier height is $V_b = k^2/16a$.

With use of the transformation described by Chan et al.,[17] the H_V part of the Hamiltonian can be written in dimensionless coordinates as

$$H_V = K(P_o^2 + \eta X^2 + X^4) \tag{5}$$

where

$$X = (8m_o a/\hbar^2)^{1/6}x \qquad K = (a\hbar^4/64m_o^2)^{1/3}$$
$$\eta = k(m_o/a^2\hbar^2)^{1/3} \qquad P_o = (8/m_o a\hbar^4)^{1/6}p_o$$

Tables of eigenvalues λ_n for the one-dimensional problem (in dimensionless units) have been published[17,18] and were recalculated and extended further by diagonalization, using 40 harmonic oscillator basis functions. The eigenvalues are

$$E_n = K\lambda_n \qquad \lambda_n = \lambda_n(\eta)$$

The calculated, one-dimensional tunneling splittings are determined by the two potential constants k and a and the effective mass m_o. It is more convenient to use the barrier height V_b and the values of $\pm x_o$ at atom 6 of the minimum energy configurations, instead of the force constants k and a. A third choice of independent parameters yields

$$m_o(\eta) = \eta/16K(\eta)x_o^2 \qquad K(\eta) = \Delta E_{01}/\Delta\lambda_{01}(\eta)$$
$$V_b(\eta) = K(\eta)\eta^2/4 \tag{6}$$

The problem thus involves three parameters to be obtained from available experimental data which includes ΔE_{01}, information about x_0 from the structure, and values of A, B, and C for $v = 0$ and $v = 1$, plus F, all for a number of isotopic species.

The change, $B_1 - B_0$, in the rotational constant B is seen to be considerable;[3b] it is too large to arise only from motion of the hydrogen-bonded H or D. Isotopic data indicate that the oxygen–oxygen separation changes with the tunneling state and this makes a large contribution to $(B_1 - B_0)$. A further contribution to $(B_1 - B_0)$ is expected to come from the displacement of carbon atoms. Thus the changes in rotational constants with tunneling state, while surely sensitive to the details of the potential surface, are not very useful in determining the barrier height with use of simple approximations.

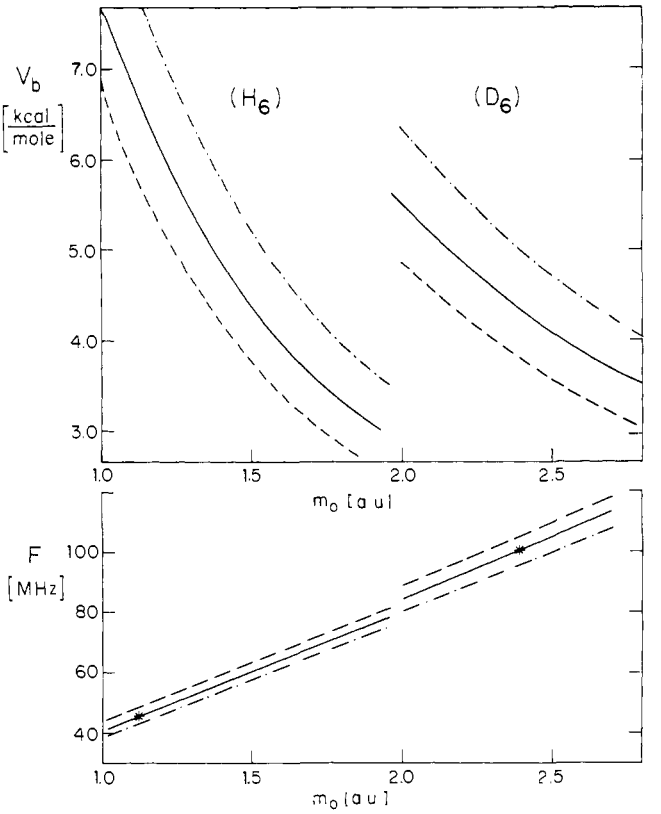

Figure 3. The upper part is the barrier, V_b, vs. effective mass, m_o, for constant tunneling splitting, ΔE_{01}, and several values of x_o. The lower plot shows the dependence of the vibrational–rotational coupling constant F on effective mass. The solid lines correspond to x_o equal to 0.375 and 0.397 Å for parent (H_6) and (D_6), respectively. The dashed lines correspond to 0.375 + 0.020 and 0.397 + 0.020 Å and the dot and dashed lines to 0.375 − 0.020 and 0.397 − 0.020 Å. The asterisks mark the experimental F values.

The off-diagonal cross product element F,[2b]

$$F = \left\langle 0 \left| \frac{\sum m_i x_i y_i}{I_a I_b - (\sum m_i x_i y_i)^2} \right| 1 \right\rangle \tag{7}$$

will be approximated by

$$F_{01} \sim [m_o y_6 \langle 0|x_6|1\rangle / I_a I_b] 505379 \tag{8}$$

if m_o is in atomic units, x and y are in angstroms and F is in MHz. The following assumptions were made:

$$\sum_i m_i x_i y_i = 0$$

at the activated state because of its presumed C_{2v} symmetry. Along the reaction path the cross-product term squared is neglected relative to $I_a I_b$ and m_6 is replaced by the effective mass m_o, even though the effective mass for F could be different from its value for ΔE_{01}. Further, constant equilibrium values of y_6 and I_a and I_b (the latter averaged over $v = 0$ and $v = 1$) were used since the fact that $\Delta A \ll \Delta B$ led to the conclusion that only x_6 has a large amplitude. Figure 3 shows the dependence upon m_o of this approximate value of F. This figure also shows plots of the barrier V_b vs. effective mass m_o for constant tunneling splitting ΔE_{01}, separately for the H_6 species and the D_6 species, for a set of values for x_o (see eq 6).

The effective mass m_o is expected to vary along the reaction path, and therefore the best approximation for it will depend on the nature of the reaction path. Probably the most important region for the calculation of the tunneling splitting ΔE_{01} is the neighborhood of the transition state at the barrier. If the reaction path there is essentially along the x_6 component of the multidi-

(15) (a) Harris, D. O.; Harrington, H. W.; Luntz, A. C.; Gwinn, W. D. *J. Chem. Phys.* **1966**, *44* 3467–3480. (b) Wieser, H.; Danyluk, M.; Kydd, R. A. *J. Mol. Spectrosc.* **1972**, *43*, 382–392. (c) Mallinson, P. D.; Mills, I. M. *Mol. Phys.* **1975**, *30*, 209–216. (d) Halonen, L; Friz, E.; Robiette, A. G.; Mills, I. M. *J. Mol. Spectrosc.* **1980**, *79*, 432–445.

(16) The ring-puckering problem is simpler to handle because several excited states of the low puckering mode can usually be identified. Also the changes in the rotational constant B seem to be accounted for by the simple puckering motion. In malonaldehyde the heavy atoms must move and the bond distances as well as the bond angles are affected by the motion. Therefore it was not possible to follow the ring-puckering treatment closely.

(17) Chan, S. I.; Stelman, D.; Thompson, L. E. *J. Chem. Phys.* **1964**, *41* 2828–2835.

(18) Chan, S. I.; Stelman, D. *J. Mol. Spectrosc.* **1963**, *10*, 278–299.

Table III. Estimates of the Barrier, V_b [kcal/mol], and Effective Mass, m_o [au]

	from F's		from κ's	
	V_b	m_o	V_b	m_o
(D_6)	4.4	2.39	5.0	2.17
(D_6D_8)	4.6	2.16	4.5	2.17
($D_6D_8{}^{18}O_1{}^{18}O_3$)	4.2	2.36	4.7	2.19
($D_6D_7D_9$)	4.0	2.53	5.0	2.16
($D_6D_7D_8D_9$)	4.2	2.31	4.6	2.17
($D_6D_8{}^{13}C_2{}^{13}C_4$)	4.8	2.12	4.6	2.17
($D_6D_8{}^{13}C_2{}^{13}C_3{}^{13}C_4$)	5.0	2.05	4.6	2.17
parent (x_O = 0.390 Å)	6.4	1.07	5.7	1.17
parent (x_O = 0.375 Å)	6.8	1.12	6.4	1.17

mensional energy surface, m_o should be ~1 for H and ~2 for D. However, it is seen in Table II that symmetrical isotopic substitutions at atoms other than atom 6 cause several percent changes in the tunneling splitting (for D_6 species). It is clear from this that the effective mass for D_6 species ought to be greater than 2.

One approach for estimating the barrier V_b is to use the experimental values of F listed in Table II to obtain values of the effective mass for the several isotopic species from Figure 3. Then, from the upper curves of Figure 3 and the effective mass, estimates of V_b can be read off. The results are listed in Table III. The values of x_o and y_6 were obtained from the structures of ($D_6D_7D_8$)[3b] rotated to the principal axes of each isotopical species. For the parent malonaldehyde this led to x_o = 0.390 Å. The second value for the normal species involved altering the O–C–C ring angles to change the O–O distance by 0.021 Å to the value indicated for H_6 species[3b] (the Ubbelohde effect), and that gave x_o = 0.375 Å. Table III shows that these calculations yield barriers ranging from 4.0 to 6.8 kcal/mol.

An alternative approach involves the formula

$$m_o = \sum m_i(l_i/l_H)^2 = \sum \kappa_i m_i \qquad (9)$$

in which l_i is the displacement of atom i associated with the displacement l_H of H_6 in the critical portion of the reaction path. The second form of this equation can be used, in conjuction with the known dependence of K, $\Delta\lambda$, and m_o on η (see Appendix), to determine the κ_i (considered as constants) from the observed tunneling splittings of an appropriate set of isotopic species:

$$\kappa_i = \frac{\delta\Delta E_{01}}{\delta m_i}\frac{3m_o}{KG(\eta)} \qquad i \neq 6\ (\kappa_6 = 1) \qquad (10)$$

where

$$\delta\Delta E_{01} = \Delta E_{01}(i) - \Delta E_{01}(D_6D_8)$$

and

$$G(\eta) = \eta\frac{d\Delta\lambda_{01}}{d\eta} - 2\Delta\lambda_{01}$$

These κ values will depend on the choice of value for V_b. Self consistency is achieved by varying V_b (hence η, K, and m_o) until m_o calculated from

$$m_o = \sum \kappa_i m_i = m_6 + \sum_{i\neq 6} \kappa_i m_i \qquad (11)$$

agrees with m_o from Figure 3. Note that $\delta\Delta E_{01}$ is the change in ΔE_{01}, relative to the reference species (here (D_6D_8)), due to a mass change δm_i at atom i or for simultaneous changes of mass at i and at the other equivalent atom.

The barrier thus found for (D_6D_8) was 4.5 kcal/mol and the corresponding effective mass was 2.17 au. When the same κ's were used for parent species, the reduced mass was 1.17 au which corresponds to V_b = 5.7 (for x_o = 0.39 Å) and V_b = 6.4 kcal/mol (for x_o = 0.375 Å). F was 49.3 and 47.5 MHz respectively, compared to the experimental value 45.5 MHz. The final κ_i's are shown in Table IV. Note that the values of V_b determined by using eq 9–11 lie within the range obtained from the F approach.

Table IV. Coefficients κ_i Determined from Equation 10

κ_6	1.0	$\kappa_7 + \kappa_9$	−0.0022
κ_8	0.0056	$\kappa_2 + \kappa_3 + \kappa_4$	0.0033
$\kappa_1 + \kappa_5$	0.0077	$\kappa_2 + \kappa_4$	0.0026

Table V. Summary of More Recent ab Initio SCF Calculations on Malonaldehyde

method	barrier, kcal/mol	O···O distance, Å	ref
	11.5	2.63	20
CI	10.0		5b
	6.6	2.56	5a
	10.3	2.56	5c
CI	9.8		5c
	11.4	2.69	8
CI	8.5		8
+ unlinked clusters	8.0		8
+ zero-point energy[a]	5.0		8

[a] See text.

These different approaches then lead to a rough value of V_b of 4.0 to 5.0 kcal/mol for deuterium tunneling species. For the parent species less data give a higher value of ~6.6 kcal/mol.

Note also that the reduced mass values in Table III lie fairly near but slightly higher than the "bare" values of 1 and 2 for H and D, respectively. Since the carbon and oxygen atoms must undergo fairly large displacements when their bonds change from single to double and vice versa as the hydrogen tunnels, the heavy-atom displacements presumably are not proportional to the hydrogen displacements in the important portion of the reaction path. Proportionality would lead to considerably larger effective masses.[2b] It will be interesting to compare this statement with reaction path calculations in the future. Rossetti and Brus[4] found a similar result for tropolone.

Note in Table IV that, except for κ for ($D_6D_7D_8D_9$) which comes out with an unacceptable negative value, the other atoms contribute roughly similar amounts, all small compared to the contribution of H_6 (or D_6) itself.

From the estimated barrier values one can also calculate from the model the energies of the next two tunneling states. For example, barriers between 4 and 7 kcal/mol lead to a pair of energy levels, the first of which is between 860 and 1420 cm^{-1} above the ground level pair and the second between 1190 and 1820 cm^{-1}. The splitting between the second and the third level should lie between 330 and 400 cm^{-1} for hydrogen tunneling. Obviously, this leads to "O–H" frequencies much lower than have been determined from empirical relations involving the O···O distance[19a] or the C=O stretching frequency.[19b]

Comparison with Theory

A number of quantum chemical calcualtions of the barrier height have been published. The more recent a priori values are listed in Table V. These values need several adjustments before comparing them with our experimental results. First, it is seen that configuration interaction, CI, lowers the SCF values while unlinked cluster terms cause a further lowering. Finally the difference of the zero-point vibrational energies for the transition state and the equilibrium configuration may lead to a further correction (which is perhaps not very reliably known since it depends entirely on the calculated vibrational frequencies for these two states).[8] The end result is somewhat encouraging, considering the many approximations and uncertainties in both the theoretical and experimental approaches.

Acknowledgment. The authors thank Dr. S. L. Coy for considerable help and advice. The financial support of the National

(19) (a) Tayyari, S. F.; Zeegers-Huyskens, T.; Wood, J. L. *Spectrochim. Acta, Ser. A* **1979**, *35A*, 1289–1295. (b) Tayyari, S. F.; Zeegers-Huyskens, T.; Wood, J. L. *Ibid.* **1979**, *35A*, 1265–1276.

(20) Karlström, G.; Wennerström, H.; Jönsson, B.; Forsen, S.; Almlöf, J.; Ross, B. *J. Am. Chem. Soc.* **1975**, *97*, 4188–4192.

Science Foundation under Grant 80-11956 is gratefully acknowledged.

Appendix

Let χ be some measurable quantity which is a function of m_o, V_b, and x_o. V_b and x_o will be held constant. Then let

$$\partial\chi/\partial m_o = f(m_o, V_b, \chi_o)$$

If l_i is the path length over which atom i moves during the tunneling displacement l_H of hydrogen H_6, then the effective mass is

$$m_o = \sum_i m_i(l_i/l_H)^2 = \sum_i m_i\kappa_i \qquad (\kappa_6 = 1)$$

where $\kappa_i = (l_i/l_H)^2$. It will be assumed that κ_i is a constant for each atomic position so that

$$\partial m_o/\partial m_i = \kappa_i$$

and

$$\delta\chi = f\delta m_o = f\kappa_i\delta m_i$$

for small δm_i so

$$\kappa_i = \frac{\delta\chi}{\delta m_i}\frac{1}{f} \text{ and } m_6 = m_o + \frac{1}{f}\sum_{i\neq 6}' m_i\frac{\delta\chi}{\delta m_i}$$

where $\delta\chi$ is the change in χ on changing the mass at position i from m_i to $m_i + \delta m_i$. If $\delta\chi$ is the change in the tunneling splitting on isotopic substitution, the equation above for m_o can serve as a tool for finding the value of m_o which yields self consistency.

For example, if $\chi = \Delta E_{01}$ where $\Delta E_{01} = K\Delta\lambda_{01}$ then

$$f_1 = \frac{\partial\Delta E_{01}}{\partial m_o} = \Delta\lambda_{01}\frac{\partial K}{\partial m_0} + K\frac{\partial\Delta\lambda_{01}}{\partial m_o}$$
$$= \frac{-2K}{3m_o}\Delta\lambda_{01} + \frac{K\eta}{3m_o}\frac{d\Delta\lambda_{01}}{d\eta}$$
$$= \frac{K}{3m_o}\left(\eta\frac{d\Delta\lambda_{01}}{d\eta} - 2\Delta\lambda_{01}\right) = f_1 \text{ (negative)}$$

Registry No. A, 64516-42-3; A-(D_6), 89066-01-3; A-(D_6D_8), 89066-02-4; A-($D_6D_8{}^{18}O_1{}^{18}O_5$), 89066-03-5; A-($D_6D_7D_9$), 89066-04-6; A-($D_6D_7D_8D_9$), 89066-05-7; A-($D_6D_8{}^{13}C_{2-4}$), 89066-06-8; A-($D_6D_8{}^{13}C_{2-4}{}^{13}C_3$), 89066-07-9; A-($D_6D_8{}^{13}C_2{}^{13}C_4$), 89066-08-0; A-($D_6D_8{}^{13}C_2{}^{13}C_3{}^{13}C_4$), 89066-09-1.

Microwave Spectroscopic Study of Malonaldehyde. 4. Vibration–Rotation Interaction in Parent Species

Paul Turner,[†1a] Steven L. Baughcum,[‡1b] Stephen L. Coy,[‡] and Zuzana Smith*[‡]

Contribution from the Departments of Chemistry, University of Reading, Reading RG6 2AD, England, and Harvard University, Cambridge, Massachusetts 02138.
Received November 18, 1983

Abstract: The microwave spectrum of the parent species of malonaldehyde, which shows Coriolis perturbations only at high J values, has been analyzed with a Hamiltonian which includes both centrifugal distortion and Coriolis terms. The Nielson/Halonen computer program, which treats the Coriolis interaction by introducing a cross term in the inverse inertial tensor, fitted 183 transitions with 20 parameters with excellent accuracy. The fit appears to be unique. Transitions up to $J = 38$ were predicted in the hitherto unexplored 74–85-GHz region. A Stark spectrometer capable of covering this region was devised, using a Raytheon QKK-866 klystron source which could be either swept or phase locked to a harmonic from the R band output of an HP 8460A microwave spectrometer. The same locking arrangement provided accurate frequency measurement. All the transitions were found within 2 MHz of predicted values (<0.5 MHz for $J < 34$). The analysis of all the data gave a tunneling splitting, ΔE_{01}, of 21.583 cm^{-1} and an inverse inertial tensor cross-term coefficient, F, of 45.5 MHz.

Paper 3[2] contains an analysis of Coriolis (or inertial cross product) perturbations in the microwave spectra of several isotopic species of gaseous malonaldehyde (3-hydroxy-1-propenal), particularly those species in which the tunneling atom is deuterium. It was pointed out that the species in which the tunneling atom is not D but H present more difficulty. From intensity measurements on the parent malonaldehyde the tunneling splitting, ΔE_{01}, was estimated to be 26 ± 10 cm^{-1},[3] so useful perturbations would only appear at higher rotational energies, which requires that centrifugal distortion terms be included in the Hamiltonian, in addition to rigid rotor and Coriolis (or inertial cross product) terms. The interaction terms are

$$H = (F + F''J)(P_aP_b + P_bP_a)$$

where F'' is quite small.

Fortunately, a program of this form became available.[4] It has the capability of fitting 34 parameters, A, B, C, Δ_J, Δ_{JK}, Δ_K, δ_J, δ_K, and sextic centrifugal distortion constants for $v = 0$ and separately for $v = 1$, plus ΔE_{01}, F, and F''.

Analysis

The Nielson/Halonen program was applied to two deuterated species, namely (D_6D_8) and ($D_6D_8{}^{13}C_2{}^{13}C_3{}^{13}C_4$), leading to tunneling splittings of 2.884 and 2.828 cm^{-1}, respectively, which agree very well with the results of the CORFIT program.[2] This program[6] includes Coriolis terms but no centrifugal distortion which limits

[†] University of Reading.
[‡] Harvard University.

(1) (a) Present address: Bruker Analytische Messtechnik GmBH, D-7512 Rheinstetten 4, Karlsruhe, West Germany. (b) Present address: Los Alamos National Laboratory, Los Alamos, NM 87545.
(2) Baughcum, S. L.; Smith, Z.; Wilson, E. B.; Duerst, R. W. *J. Am. Chem. Soc.*, preceding paper in this issue.
(3) Baughcum, S. L. Ph.D. Thesis, Harvard University, 1978.
(4) This program was originally written by C. J. Nielsen,[5] considerably modified by L. Halonen, and successfully used by the following: Halonen, L.; Friz, E.; Robiette, A. G.; Mills, I. M. *J. Mol. Spectrosc.* **1980**, *79*, 432–445.
(5) Nielsen, C. J. *Acta Chem Scand.* **1977**, *31*, 791–792.
(6) Pickett, H. M., Jet Propulsion Laboratory, California Institute of Technology, Pasadena CA 91109.

0002-7863/84/1506-2265$01.50/0